

# 6085

International Symposium on Room Air Convection and Ventilation Effectiveness  
University of Tokyo, July 22 - 24, 1992



**Numerical Simulation of Velocity and Temperature Fields  
within Atrium based on Modified  $k-\epsilon$  Model  
Incorporating Damping Effect due to Thermal Stratification**

Tomoyuki Chikamoto  
*University of Tokyo, Japan*

Shuzo Murakami  
*IIS, University of Tokyo, Japan*

Shinsuke Kato  
*IIS, University of Tokyo, Japan*

**ABSTRACT**

Thermally stratified flow and temperature fields within an atrium were analyzed by a modified  $k-\epsilon$  model. The modified model proposed here incorporates damping effect on vertical turbulent transport due to thermal stratification. New wall functions for wall boundary condition were derived with reference to the DNS data base of weak shear layer of couette flow [1]. A model experiment for the same atrium was also conducted and the results of the experiment were compared with those of the simulation. The agreement between the numerical simulation and the model experiment was fairly good. A highly-stable temperature field was well reproduced by means of the modified  $k-\epsilon$  model and the new wall functions.

**KEYWORDS** Atrium, Thermal Stratification, Laminarization,  $k-\epsilon$  model, Wall function, Room airflow

**INTRODUCTION**

Today many architects all over the world desire to include atria or similar glass-covered spaces in their buildings. It is very difficult to predict and control the indoor climate in such spaces because of their large sizes and rather heavy heat loads. Sunshine and heat penetrate the glazed roofs and often leave the flowfields in the atria thermally stratified and roughly laminar. This thermal stratification suppresses the vertical flux of heat and momentum and also decreases the turbulence intensity of the flowfield. Thus, the vertical temperature gradient becomes very large. In the design of air-conditioning systems for those spaces, it is important to predict the effect of thermal stratification on velocity and temperature distributions. However, there are few experimental methods for systematically assessing flow and temperature fields in atria and also few useful numerical techniques for predicting highly-stratified flowfields precisely. The purpose of this study is to propose a new turbulence model which can predict velocity and temperature fields within a highly-stratified atrium with ease and sufficient accuracy. In this study, experiments using a model atrium space (1/20 scale model of a 24m x 12m x 24m space) were also conducted and the results were compared with those of numerical simulation.

The standard  $k-\epsilon$  model [2] is a very useful model and has yielded reasonable solutions not only in isothermal but also in non-isothermal flowfields. However the  $k-\epsilon$  model does not always lead to accurate and stable results in the simulation of an atrium space with strong thermal stratification. Since this model is very simple and popular, it would be very useful and practicable if

some modification could overcome the difficulties in analyzing the flowfield in an atrium. In this study more elaborate turbulence models such as DSM (Differential Stress Model) and ASM (Algebraic Stress Model) were not used. When modifying the  $k-\epsilon$  model, the following flowfield conditions were considered.

- (1) In a thermally stratified flow, kinematic energy is suppressed greatly due to negative buoyancy effect.
- (2) Since the standard  $k-\epsilon$  model was originally developed for analyzing a fully turbulent flow, it does not function satisfactorily in analyzing a laminar flowfield. Although various low-Reynolds number  $k-\epsilon$  models have been developed for analyzing the near-wall region (viscous and buffer layer) of the wall boundary layer [3], they may not be used for a roughly laminar flowfield apart from a wall. Most of the previous methods of numerical analyses in which buoyancy effect is incorporated have not been successful when applied to highly-stratified and roughly-laminar flowfields [4, 5, 6].

**Table 1 Basic Equations of the Modified  $k-\epsilon$  Model Incorporating Damping Effect of Laminarization and Thermal Stratification**

(Momentum-eq.)	$\frac{DU_i}{Dt} = -\frac{1}{\rho} \frac{\partial P}{\partial x_i} + \frac{\partial}{\partial x_j} (\nu \frac{\partial U_i}{\partial x_j} - \overline{u_i u_j}) - g_i \beta \Theta$	(1)
( $k$ -eq.)	$\frac{Dk}{Dt} = D_k + P_k + G_k - \epsilon$	(2)
( $\epsilon$ -eq.)	$\frac{D\epsilon}{Dt} = D_\epsilon + \frac{\epsilon}{k} (C_{\epsilon 1} P_k + C_{\epsilon 2} G_k - C_{\epsilon 3} \epsilon)$ (cf. note 1)	(3)
( $\Theta$ -eq.)	$\frac{D\Theta}{Dt} = \frac{\partial}{\partial x_j} (\frac{\nu}{Pr} \frac{\partial \Theta}{\partial x_j} - \overline{u_j \Theta})$	(4)
	$P_k = -\overline{u_i u_j} \frac{\partial U_i}{\partial x_j}$ (5)	$G_k = -g_i \beta \overline{u_i \Theta}$ (6)
	$D_k = \frac{\partial}{\partial x_j} \{ (\nu + \frac{\nu_t}{\sigma_k}) \frac{\partial k}{\partial x_j} \}$ (7)	$D_\epsilon = \frac{\partial}{\partial x_j} \{ (\nu + \frac{\nu_t}{\sigma_\epsilon}) \frac{\partial \epsilon}{\partial x_j} \}$ (8)
	$\overline{u_i u_j} = -\nu_t (\frac{\partial U_i}{\partial x_j} + \frac{\partial U_j}{\partial x_i}) + \frac{2}{3} k$ (cf. note 2) (9)	$\overline{u_i \Theta} = -\frac{\nu_t}{\sigma_\theta} \frac{\partial \Theta}{\partial x_i}$ (cf. note 2) (10)
	$\nu_t = C_\mu f_\mu \frac{k^2}{\epsilon}$ (11)	$f_\mu = f_B \cdot f_{Rt}$ (12)
	$f_{Rt} = \exp\left\{ \frac{-3.4}{(1+Rt/50)^2} \right\}$ [ref. 8] (13)	
	$f_B : 0.0 (B \leq \frac{1}{a_0}), \quad 1 - a_0 \cdot B (\frac{1}{a_0} < B < 0), \quad 1.0 (0 \leq B) ; B = G_k/\epsilon$ [ref. 9] (14)	
	$\sigma_k: 1.0 \quad \sigma_\epsilon: 1.3 \quad \sigma_\theta: 0.9 \quad C_\mu: 0.09 \quad C_{\epsilon 1}: 1.44 \quad C_{\epsilon 2}: 1.92 \quad C_{\epsilon 3}: 1.44 (G_k > 0), 0.0 (G_k \leq 0) \quad a_0 = -0.1$	

#### <Nomenclature>

$U_i$ : average velocity component in $i$ direction	$f_\mu$ : damping function ( $f_B \cdot f_{Rt}$ )
$u_i$ : fluctuating velocity component in $i$ direction	$f_B$ : damping function of $B$
$k$ : turbulence energy	$f_{Rt}$ : damping function of $Rt$
$\epsilon$ : dissipation of turbulence energy $k$	$U_w$ : velocity of moving wall
$\Theta$ : average value of temperature	$\tau_w$ : wall shear stress
$\theta$ : fluctuation of temperature	$u^*$ : friction velocity
$P_k$ : generation term of $k$ due to mean shear	(subscript: $m$ ; moving wall, $f$ ; fixed wall)
$G_k$ : generation term of $k$ due to buoyancy	$u'$ : dimensionless velocity
$\nu_t$ : eddy kinematic viscosity	$y'$ : dimensionless distance from wall ( $u^* \cdot y/\nu$ )
$\nu$ : kinematic viscosity	$g_i$ : gravitational acceleration in $i$ direction
$B$ : buoyancy parameter ( $G_k/\epsilon$ )	Pr: Prandtl number
$Rt$ : turbulent Reynolds number ( $k^2/\nu \cdot \epsilon$ )	$\beta$ : coefficient of volumetric expansion
$Rf$ : flux Richardson number ( $-G_k/P_k$ )	$\delta_{ij}$ : Kronecker delta



(3) In a thermally stratified flowfield,  $\nu_t$ , which is based on the gradient transport hypothesis, should be adjusted by Richardson number, Reynolds number and Prandtl number in order to deal with the damping effects of turbulence transport in the vertical direction [7].

In this paper, a new type  $k-\epsilon$  model which incorporates the damping effect due to stratification and laminarization are proposed. It is here called the "non-near-wall type, low-Reynolds number  $k-\epsilon$  model." The phrase "non-near-wall type, low Reynolds number" indicates that the model is applicable also to a roughly-laminar flow apart from a wall. A rather coarse mesh system was used at the region near the wall in this study. In order to bridge the wall surface and the flow properties at the near wall cell, new wall functions were used as the boundary condition; these were derived with reference to the DNS (Direct Numerical Simulation) data base of the weak shear layer near the moving wall of a couette flow (ref. [1], cf. note 3).

### SPECIFICATION OF ATRIUM USED (Figure 1)

A simple model of a rectangular atrium ( $X_1:24m \times X_2:12m \times X_3:24m$ ) is used [10]. Figure 1 shows a schematic view of the model atrium. The ceiling and the floor are heated in order to reproduce the effect of sunshine. A convective heat flux from each wall surface is given for the simulation.

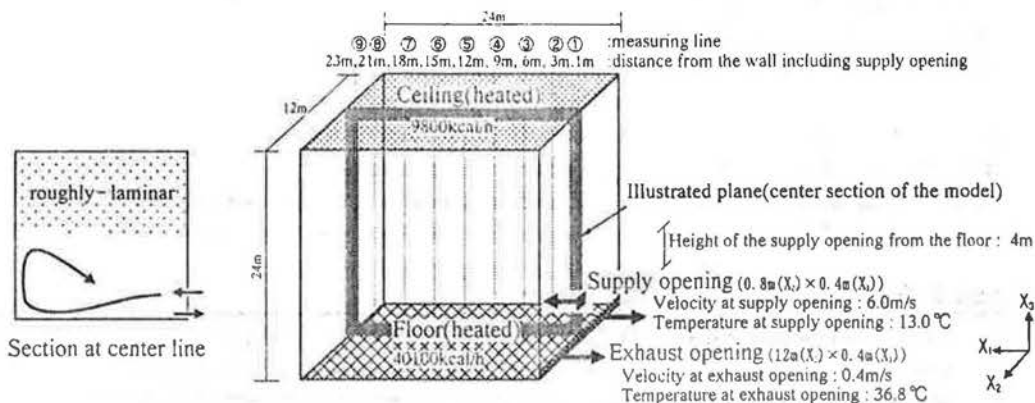


Figure 1 Model atrium used for simulation and experiment (numbers are real scale; in experiment 1/20 scale model was used)

Table 2 Boundary conditions

Supply opening	$U_{in}=6.0\text{m/s}$ , $k_{in}=1/2 \cdot (U_{in} \times 0.1)^2$ $\epsilon_{in}=C_{\mu} \cdot k_{in}^{3/2} / l_{in}$ ( $l_{in}=0.4\text{m}$ ), $\Theta_{in}=13.0^\circ\text{C}$
Exhaust opening	$U_{out}=0.4\text{m/s}$ , $k_{out}, \epsilon_{out}, \Theta_{out}$ : free slip condition
Wall boundary	The wall shear stress $\tau_{wm}$ is given by equation ①. The value of $k$ at the first near-wall node is expressed by equation ②. The value of $\epsilon$ at the first near-wall node is expressed by equation ③ (cf. note 3). $\frac{U_1}{\sqrt{\tau_{wm}/\rho}} = \begin{cases} y' \cdot (y' \leq 2), & -0.040(y')^2 + 0.89y' + 0.17 \quad (2 < y' \leq 10) \\ 3.6(y')^{1/7} & (10 < y') \end{cases} \quad \text{①}$ $\frac{k}{\tau_{wm}/\rho} = \begin{cases} 0.00022(y')^2 - 0.018(y')^2 + 0.58y' & (y' \leq 10) \\ 39(y')^{-1} & (10 < y') \end{cases} \quad \text{②}$ $\frac{\nu \epsilon}{(\tau_{wm}/\rho)^2} = \begin{cases} 0.012(y')^2 - 0.068y' + 0.78 & (y' \leq 10) \\ 17(y')^{-2} & (10 < y') \end{cases} \quad \text{③}$ $y' = \frac{\sqrt{\tau_{wm}/\rho} \cdot y}{\nu} \quad \text{④}$ Heat flux at heated wall is given according to the experimental condition (cf. Figure 1), at other wall it is 0.0.

## OUTLINE OF MODIFIED $k-\varepsilon$ MODEL

The basic equations for the modified  $k-\varepsilon$  model are shown in Table 1.

### (1) Basic concept for developing new model

- ① This model was developed as a "non-wall type, low-Reynolds number model". It aims to reproduce a roughly-laminar flowfield not only near a wall but also apart from a wall.
- ② Damping effect by buoyancy which leads to laminarization is incorporated into the expression of  $\nu_t$  by introducing damping function  $f_\mu$ . Reduction of the value of  $\nu_t$  leads to decrease of Reynolds stress and turbulence heat flux in the vertical direction and consequently damps the production of turbulence energy  $k$ .

### (2) Damping function $f_\mu (=f_b \times f_{ri})$ (Table 1, eq. (11) ~ (14))

Buoyancy parameter  $B (=G_k/\varepsilon)$  [9], and turbulence Reynolds number (laminarization parameter)  $Rt (=k^2/\nu\varepsilon)$  are used for scaling the damping effect on  $\nu_t$  (cf. note 4). Damping effect by  $B$  is given linearly through  $f_b$ , i.e.  $f_b \sim B$  (cf. Table 1, eq. (14)). In a highly-stratified flowfield,  $B$  shows a large negative value and thus  $f_b$  becomes nearly 0. On the other hand, under an unstable condition,  $B$  is positive and  $f_b$  equals 1.  $f_{ri}$  is the model proposed by Launder and Sharma [8]. When the flowfield becomes laminar,  $Rt$  goes to 0 and  $f_{ri}$  approaches 0.033. When the flow becomes turbulent,  $f_{ri}$  converges to 1 according to the increase of  $Rt$ .

### (3) Boundary conditions (Table 2)

Although the "low-Reynolds number"  $k-\varepsilon$  model is used, this model is not designed to incorporate the damping effect due to a solid wall. In this simulation, the mesh dividing near the wall is not fine enough to use no-slip type boundary conditions. Wall functions which reflect the flowfield of the near-wall sublayer were used to determine the boundary conditions. The flow property near a wall in case of room air flow is greatly different from that of channel flow. In the case

**Table 3 Grids and schemes for calculation**

The computational domain is discretized into  $35 (X_1) \times 17 (X_2) \times 45 (X_3)$  (cf. Figure 1). The side of the supply opening is divided into 4 grids in  $X_2$  direction and 2 grids in  $X_3$  direction. One-half space of  $X_2$  direction was calculated, considering the symmetrical property of the flowfield. The convection term of  $U_i$  was calculated by means of the QUICK scheme. The convection terms of  $k$ ,  $\varepsilon$  and  $\Theta$  were calculated by means of the QUICK scheme, except for the area just around the supply and exhaust openings, where the first-order upwind scheme was used.

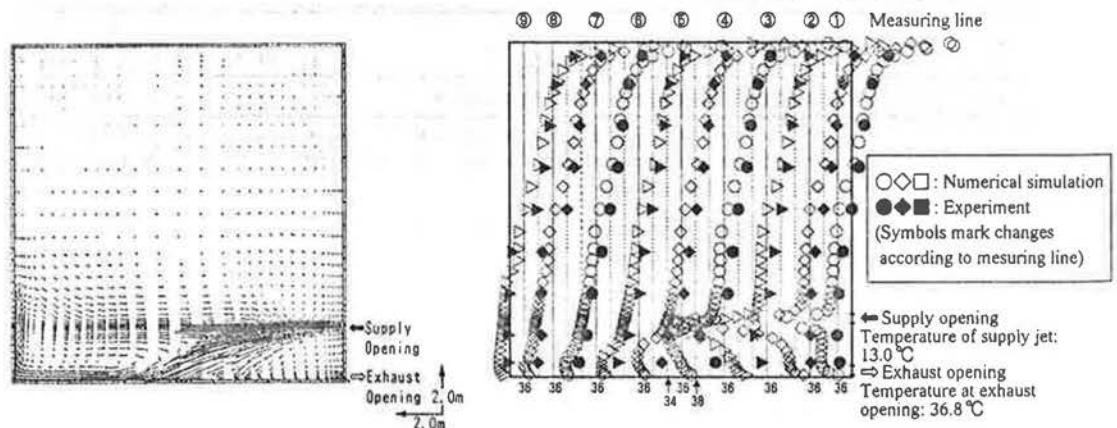


**Figure 2 Distribution of velocity vectors (center section)**

**Figure 3 Vertical distribution of temperature**

of a thermally stratified flowfield, it often becomes roughly-laminar. Here the wall functions used for the boundary condition were derived with reference to the DNS data base of the weak shear layer of a couette flow. The wall functions are shown in Table 2, and details are described in note 3. Grids and schemes for calculation are shown in Table 3.

## RESULTS AND DISCUSSION

The modified  $k-\epsilon$  model succeeds in giving a stationary solution of a highly-stratified and roughly-laminar flowfield whereas the standard, high-Reynolds number  $k-\epsilon$  model failed to obtain it (cf. note 5).

The results of the numerical simulation are compared with those of the experiment. Figure 4 shows the flow visualization of the model experiment, in which smoke is injected into the supply air. In the experiment, an apparent thermal stratification is observed. The cold supply air does not rise to half of the atrium height. In the thermally stratified layer, especially at the boundary between the smoked and non-smoked regions, a gravity wave is observed in the model experiment.

### (1) Distribution of velocity (Figure 2)

The distribution of velocity vectors in the central vertical section is illustrated in Figure 2. The

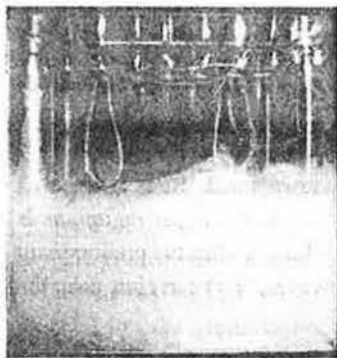


Figure 4 Flow visualization (smoke is injected in supply air, center section, model experiment)

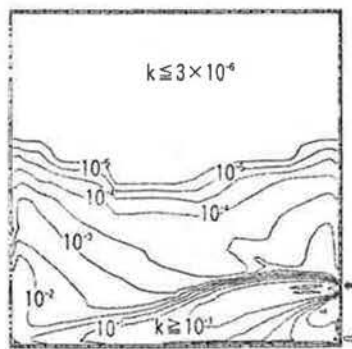


Figure 5 Distribution of turbulence energy  $k$

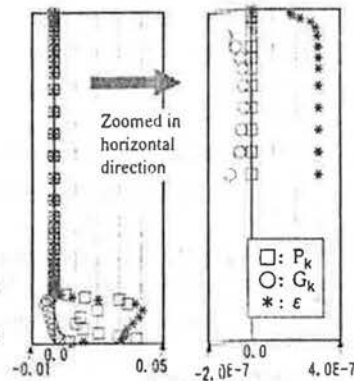


Figure 6 Comparison of  $P_k$ ,  $G_k$  and  $\epsilon$

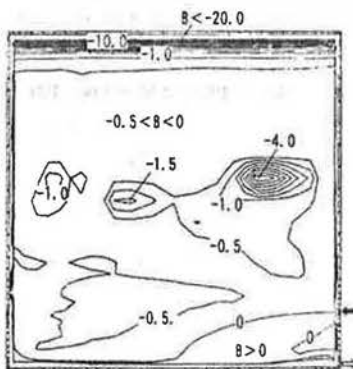


Figure 7 Distribution of  $B$

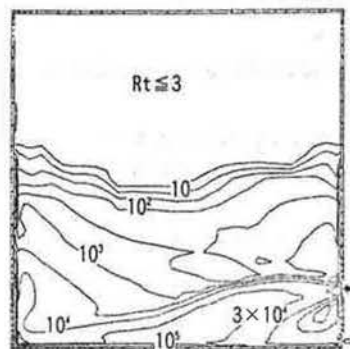


Figure 8 Distribution of  $Rt$

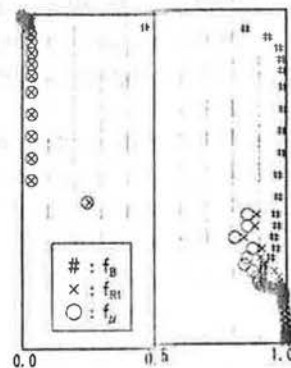


Figure 9 Comparison of  $f_b$ ,  $f_{Rt}$  and  $f_v$  (measuring line ⑤)



cold jet from the supply opening descending to the floor due to negative buoyancy effect, collides with the opposite wall. It rises along the wall and then moves downward again. The supplied air does not mix with the air in the upper region of the atrium. In the upper region of the space, it is stagnant. The value of scalar velocity ( $\sqrt{U_1^2 + U_2^2 + U_3^2}$ ) is less than 5 cm/s in this region.

**(2) Distribution of temperature (Figure 3)**

The mean temperature distributions are compared in Figure 3. Thermal stratification is clearly observed in these distributions. In particular, the temperature distribution is very large in the region near the ceiling. Agreement between the numerical simulation and the model experiment is generally satisfactory.

**(3) Distribution of turbulence energy  $k$  (Figure 5)**

In the upper region where the supply jet does not reach, turbulence decays and the value of turbulence energy  $k$  becomes very small. It is almost zero in the upper half of the model atrium ( $k \leq 3 \times 10^{-4}$ ). This modified  $k-\epsilon$  model thus succeeds in reproducing a roughly-laminar flowfield while the standard  $k-\epsilon$  model fails to do so (cf. note 5).

**(4) Comparison of  $P_k$  (generation term of  $k$  due to mean shear),  $G_k$  (generation term of  $k$  due to buoyancy) and  $\epsilon$  (dissipation term of  $k$ ) (Figure 6).**

In the upper region of the atrium,  $P_k$ ,  $G_k$  and  $\epsilon$  become negligibly small. Compared with  $G_k$  and  $\epsilon$ ,  $P_k$  is much closer to 0 in this region.  $Rf (= -G_k/P_k)$  therefore fluctuates largely and cannot be used to judge the degree of stratification (cf. note 4).

**(5) Distribution of buoyancy parameter  $B$  (Figure 7)**

In the region where the supply jet does not reach,  $B$  is negative. The negative value of  $B$  becomes very large near the ceiling, and thereby  $\nu_t$  is very much damped in this region (Figure 9).

**(6) Distribution of turbulent Reynolds number  $Rt$  (Figure 8)**

In the upper region where the supply jet does not reach,  $Rt$  becomes small.  $Rt$  is defined as  $k^2/\nu\epsilon = 1/C_\mu \cdot \nu_t/\nu \approx 10 \cdot \nu_t/\nu$ . Consequently here  $\nu_t$  is about 1/3 of  $\nu$  in the upper region, as is shown in Figure 8.  $\nu_t$  is damped in the whole upper part of the atrium. Thus  $f_{Rt}$  has the predominant effect on damping function  $f_\mu (= f_b \times f_{Rt})$  in almost all regions. However, in the region near the ceiling,  $f_\mu$  decreases to zero because  $f_b$  becomes zero (Figure 9).

**CONCLUSION**

- ① A new modified  $k-\epsilon$  model was proposed, one which incorporates damping effect and can reproduce the suppression of turbulence transport and decay of turbulence energy  $k$  caused by high-stratification and laminarization.
- ② New wall functions for wall boundary condition were derived with reference to DNS data base of weak shear layer of couette flow.
- ③ The correspondence between the results of the simulation and those of the experiment were fairly good.
- ④ In the model atrium, the temperature gradient in the vertical direction becomes very large.
- ⑤ In the upper region of the space, the turbulence Reynolds number  $Rt$  becomes very small and the flow is roughly-laminar.
- ⑥ A highly-stratified flowfield in a room is stagnant and roughly-laminar, and turbulence energy  $k$  becomes very small. These phenomena are well reproduced by the modified  $k-\epsilon$  model.

**NOTES**

1. In this model, a Viollet type model [11] is used for the estimation of the production term by buoyancy in the transport equation for  $\epsilon$  (Table 1, eq. (3)). In the Viollet type model, when  $G_k$  becomes positive, this production term by buoyancy has the same coefficient as that of the

production term by mean shear (namely  $C_{\epsilon 3} = C_{\epsilon 1}$ ), and when  $G_k$  becomes negative, it is negated ( $C_{\epsilon 3} = 0$ ). This Viollet type model produces  $\epsilon$  by buoyancy production and suppresses the unrealistic increase of  $k$  in the unstable region. These properties do not conflict with the concept of the modification of the model in this paper.

2. The eddy viscosity model is used in this model to estimate Reynolds stress  $\overline{u_i u_j}$  and turbulent heat flux  $\overline{u_i \theta}$ . However many researchers have reported that the isotropic eddy viscosity model is not adequate for application to a flowfield where Reynolds stress and turbulent heat flux is significantly anisotropic. Therefore, we are now examining some modifications to eddy viscosity modeling which incorporate the suppression of turbulence transport in the vertical direction due to buoyancy effect.

3. At a boundary layer in a ventilated room, the production term of  $k$  ( $P_k$ ) is generally small compared with the boundary layers in a pipe or a channel because the velocity gradient at a wall is usually very small in a room airflow. In particular, in the upper region of this atrium,  $P_k$  becomes negligibly small and it is roughly - laminar. In such boundary layers in an enclosed space, turbulence energy generated near a solid boundary is very small and usually it is transported there from a region far from the wall such as the mixing region of recirculating flow, e.g. the region around the supply jet. On the other hand, the generalized log law [2], which is widely used in the standard  $k-\epsilon$  model, was developed for analyzing flowfields with usual boundary layers in which the production term of  $k$  near the wall is large, e.g. that of channel flow. Consequently the generalized log law is not suitable for analyzing boundary layer flows with weak  $k$ - production in an enclosed space. Thus, new wall functions are deduced empirically with reference to the DNS data base of the boundary layer near the moving wall of a couette flow (Figure 10), where production of  $k$  is rather small. The distributions of  $u$ ,  $k$  and  $\epsilon$  are shown in Figures 11, 12 and 13. The production of  $k$  near the moving wall is very small. In the region close to the moving wall,  $u^+$  increases linearly with  $y^+$ . In the turbulent region near the moving wall,  $u^+$  is expressed as a power law type function of  $y^+$ . Between these two regions,  $u^+$  is given from a Lagrange's interpolation

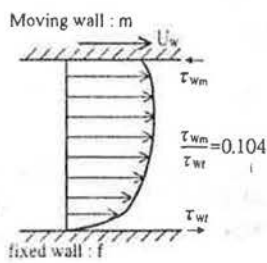


Figure 10 Couette flow

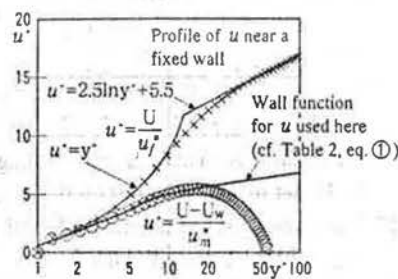


Figure 11 Velocity distribution

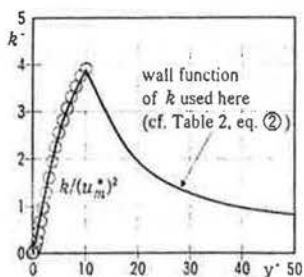


Figure 12 Distribution of  $k$

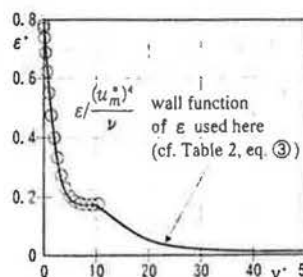


Figure 13 Distribution of  $\epsilon$

polynomial.  $k$  and  $\epsilon$  in the region near the moving wall are also given from the Lagrange's interpolation.

4. When  $P_k$  becomes much smaller than  $G_k$  or  $\epsilon$ , turbulent flow properties may be

determined mainly by  $G_k$  and  $\epsilon$  rather than by  $P_k$ . In this case,  $Rf (= -G_k / P_k)$  fluctuates greatly because of the negligibly small value of  $P_k$  and thus cannot be a good measure for judging the degree of stratification. Therefore, we adopt  $B (=G_k / \epsilon)$  as the parameter for judging stratification [8].

5. In this study, a solution of the standard  $k-\epsilon$  model was obtained only when small values of  $k$  and  $\epsilon$  were imposed at the roughly-laminar area. If the calculated values of  $k$  and  $\epsilon$  go below imposed values, calculated values must be substituted by these imposed small values. Although a stationary solution can be obtained by using this technique, it is not rational from the view point of fluid physics since the flow properties depend greatly on the imposed small values of  $k$  and  $\epsilon$ .

#### ACKNOWLEDGEMENT

We have used the DNS data base given in "Establishment of the Direct Numerical Simulation Data Bases of Turbulent Transport Phenomena" by Prof. N. Kasagi (Univ. of Tokyo) et al. The numerical data of couette flows used in this paper were given by Dr. A. Kuroda (Univ. of Hokkaido). In developing the modified  $k-\epsilon$  model, discussion with Dr. Mochida (IIS, Univ. of Tokyo) was most fruitful. The model experiment was carried out in cooperation with Mr. Yokoi (Taisei Corp.). The authors would like to express their gratitude to all of the above for their kind cooperation.

#### REFERENCES

- [1]Kuroda, A., Kasagi, A. and Hirata, M. "A Direct Numerical Simulation of the Turbulent Flow between Two Parallel Walls : Turbulence Characteristics near the Wall without Mean Shear." 5th Symposium on Numerical Simulation of Turbulence, IIS, University of Tokyo (1990), pp. 1-5
- [2]Launder, B. E. and Spalding, D. B. "The Numerical Computation of Turbulent Flows" Computer Methods in Applied Mechanics and Engineering 3 (1974), pp. 269-289
- [3]Nagano, Y., Tagawa, M. and Niimi, M. "An Improvement of the  $k-\epsilon$  Turbulence Model." J. of JSME, Vol. 55-512(B) (1989), pp. 1008-1015
- [4]Sagara, K. "On the Calculation of Turbulent Flow under Gravitational Influence." J. of AIJ, Vol. 305 (1981), pp. 88-96
- [5]Yoshizawa, A. "Statistical Modeling of Turbulent Thermally Buoyant Flow." J. Phys. Soc. Jpn. 55-9 (1986), pp. 3066-3072
- [6]Murakami, S., Kato, S. and Nakagawa, H. "Numerical Prediction of Horizontal Nonisothermal 3-D Jet in Room Based on the  $k-\epsilon$  Model." ASHRAE Transactions, V. 97, Pt. 1 (1991)
- [7]Yamakawa, M. "Statistical Modeling of Non-isothermal Turbulent Flow and Its Application." Dr. Eng. Thesis, Univ. of Tokyo, 1991
- [8]Launder, B. E. and Sharma, B.I. "Application of Energy-Dissipation Model of Turbulence to the Calculation of Flow near a Spinning Disc." Letters in Heat and Mass Transfer, Vol. 1 (1974), pp. 131-138
- [9]Launder, B. E. "On the Effects of a Gravitational Field on the Turbulent Transport of Heat and Momentum." J. Fluid Mech. Vol. 67-3 (1975), pp. 569-581
- [10]Chikamoto, T., Yokoi, M., Murakami, S. and Kato, S. "Study on Velocity and Temperature Distributions within Atrium Space (part 2 and 3)." 1991 SHASE Annual Technical Meeting, pp. 517-524
- [11]Viollet, P. L. "The Modelling of Turbulent Recirculating Flows for the Purpose of Reactor Thermal-Hydraulic Analysis." Nuclear Engineering and Design 99 (1987), pp. 365-377